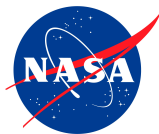


Central Compact Schemes provided with Inverse Lax-Wendroff inflow boundary condition: Stability analysis

F. Vilar¹ and C.-W. Shu¹

¹Brown University, Division of Applied Mathematics
182 George Street, Providence, RI 02912

September 26th, 2013



- 1 Introduction
- 2 Central Compact Schemes
- 3 Boundary conditions
- 4 G-K-S theory
- 5 Eigenvalue spectrum
- 6 Conclusion

- 1 Introduction
- 2 Central Compact Schemes
- 3 Boundary conditions
- 4 G-K-S theory
- 5 Eigenvalue spectrum
- 6 Conclusion

NASA project

- Wei Wang (Florida Univ.) and Mark H. Carpenter (NASA Techn. Monitor)
- Design efficient and highly accurate solvers both for direct numerical simulations and simulations of compressible flows with turbulence models

Requirements

- Good wave resolution
- High order of accuracy
- Low dissipation error

Compact schemes

- Handle non-periodic boundary conditions a lot more easily than spectral methods could
- Much smaller numerical dispersion and dissipation errors than finite difference schemes of the same order of accuracy on the same mesh

Possible issues at the boundaries

- Several ghost points near the boundary due to the wide numerical stencil
- Grids points not located on the physical boundary
- Ghost and grid points not symmetrically located with respect to the wall

Outflow boundary condition: Lagrangian extrapolation

- Ensure stability at the outflow
- Maintain the order of accuracy

Inflow boundary condition: Inverse Lax-Wendroff

- Taylor expansion of the expected order at the boundary
- Use repeatedly the partial equation (PDE) to convert the successive normal derivatives into time derivatives of the boundary condition
- Maintain the order of accuracy



S. TAN AND C.-W. SHU, *Inverse Lax-Wendroff procedure for numerical boundary conditions of conservation laws*. JCP, 2010.

- 1 Introduction
- 2 Central Compact Schemes**
- 3 Boundary conditions
- 4 G-K-S theory
- 5 Eigenvalue spectrum
- 6 Conclusion

Conservation laws

- We consider the solution of the conservation law

$$\frac{\partial u}{\partial t} + \frac{\partial f(u)}{\partial x} = 0$$

- A semidiscrete finite difference can be represented as

$$\left(\frac{\partial u}{\partial t} \right)_i = -f(u)_i^x,$$

where $f(u)_i^x$ is the approximation of $\frac{\partial f(u)}{\partial x}$ at the grid node x_i

Lele's compact schemes (JCP 1992)

- Cell-centered compact scheme (CCCS)

$$\beta f_{i-2}^x + \alpha f_{i-1}^x + f_i^x + \alpha f_{i+1}^x + \beta f_{i+2}^x = a \frac{f_{i+\frac{1}{2}} - f_{i-\frac{1}{2}}}{\Delta x} + b \frac{f_{i+\frac{3}{2}} - f_{i-\frac{3}{2}}}{3\Delta x} + c \frac{f_{i+\frac{5}{2}} - f_{i-\frac{5}{2}}}{5\Delta x}$$

- Cell-node compact scheme (CNCS)

$$\beta f_{i-2}^x + \alpha f_{i-1}^x + f_i^x + \alpha f_{i+1}^x + \beta f_{i+2}^x = a \frac{f_{i+1} - f_{i-1}}{2\Delta x} + b \frac{f_{i+2} - f_{i-2}}{4\Delta x} + c \frac{f_{i+3} - f_{i-3}}{6\Delta x}$$

Lele's cell-centered compact scheme

- The resolution of the CCCS is much better than the CNCC
- Stencil contains both the grid points and half grid points
- Only the values at the cell-centers are used to calculate the derivatives at the cell-nodes

Half grid points

- Interpolation from the values at the grid points by a compact formula

$$\beta \widehat{f}_{i-\frac{5}{2}} + \alpha \widehat{f}_{i-\frac{3}{2}} + \widehat{f}_{i+\frac{1}{2}} + \alpha \widehat{f}_{i+\frac{3}{2}} + \beta \widehat{f}_{i+\frac{5}{2}} = a \frac{f_{i+1} + f_i}{2} + b \frac{f_{i+2} + f_{i-1}}{2} + c \frac{f_{i+3} + f_{i-2}}{2}$$

- Introduce transfer errors
- Significantly reduces the resolution for high wave numbers



S.K. LELE, *Compact finite difference schemes with spectral-like resolution*. JCP, 1992.

Main idea

- If both cell-node and cell-center values are used to compute the derivatives, one could get higher order of accuracy and better resolution

New class of central compact schemes

- Central Compact Schemes (CCS)

$$\begin{aligned} & \beta f_{i-2}^x + \alpha f_{i-1}^x + f_i^x + \alpha f_{i+1}^x + \beta f_{i+2}^x \\ & = \\ & a \frac{f_{i+\frac{1}{2}} - f_{i-\frac{1}{2}}}{\Delta x} + b \frac{f_{i+1} - f_{i-1}}{2\Delta x} + c \frac{f_{i+\frac{3}{2}} - f_{i-\frac{3}{2}}}{3\Delta x} + d \frac{f_{i+2} - f_{i-2}}{4\Delta x} + e \frac{f_{i+\frac{5}{2}} - f_{i-\frac{5}{2}}}{5\Delta x} \end{aligned}$$

- Both CCCS and CNCS of Lele are special cases of these CCS



X. LIU, S. ZHANG, H. ZHANG AND C.-W. SHU, *A new class of central compact schemes with spectral-like resolution I: Linear schemes*. JCP, 2013.

Half grid points

- Stored as independent computational variables
- Computed using the same scheme, shifting the indices by $\frac{1}{2}$

$$\beta f_{i-\frac{3}{2}}^x + \alpha f_{i-\frac{1}{2}}^x + f_{i+\frac{1}{2}}^x + \alpha f_{i+\frac{3}{2}}^x + \beta f_{i+\frac{5}{2}}^x$$

$$a \frac{f_{i+1} - f_i}{\Delta x} + b \frac{f_{i+\frac{3}{2}} - f_{i-\frac{1}{2}}}{4\Delta x} + c \frac{f_{i+2} - f_{i-1}}{3\Delta x} + d \frac{f_{i+\frac{5}{2}} - f_{i-\frac{3}{2}}}{4\Delta x} + e \frac{f_{i+3} - f_{i-2}}{5\Delta x}$$

Outcome

- Gain in accuracy and resolution
- Double memory requirement in 1D
- **But same cost as compact interpolation**

Reformulation on a twice more refined mesh

- CCS rewrite as cell-node compact schemes as

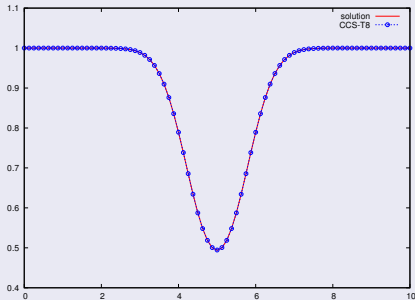
$$\beta f_{i-4}^x + \alpha f_{i-2}^x + f_i^x + \alpha f_{i+2}^x + \beta f_{i+4}^x$$

$$a \frac{f_{i+1} - f_{i-1}}{2\Delta x} + b \frac{f_{i+2} - f_{i-2}}{4\Delta x} + c \frac{f_{i+3} - f_{i-3}}{6\Delta x} + d \frac{f_{i+4} - f_{i-4}}{8\Delta x} + e \frac{f_{i+5} - f_{i-5}}{10\Delta x}$$

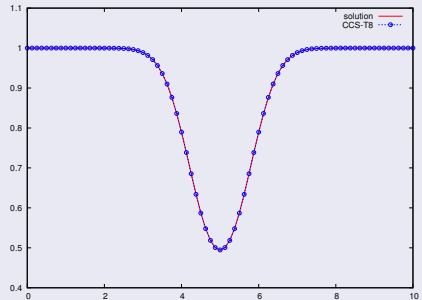
Time discretization

- Third-order TVD Runge-Kutta

Two dimensional Euler equations



(a) Final time $t = 50$



(b) Final time $t = 200$

Figure : The distribution of the density along $x = 5$ for the two dimensional advection of an isentropic vortex on a 80×80 Cartesian grid, with CCS-T8.

- 1 Introduction
- 2 Central Compact Schemes
- 3 Boundary conditions**
- 4 G-K-S theory
- 5 Eigenvalue spectrum
- 6 Conclusion

Initial Boundary Value Problem (IBVP)

- We consider the following initial boundary value problem

$$\begin{cases} \frac{\partial u}{\partial t} + \frac{\partial f(u)}{\partial x} = 0, & x \in [x_A, x_B], t \geq 0, \\ u(x_A, t) = g(t), & t \geq 0, \\ u(x, 0) = u_0(x), & x \in [x_A, x_B] \end{cases}$$

- We assume $f'(u(x_A, t)) > 0$ and $f'(u(x_B, t)) > 0$, where $f'(u) = \frac{df(u)}{du}$

Cartesian grid

- Uniform mesh $\{x_j\}_{j=0, \dots, n}$ such as

$$x_0 - C_A \Delta x = x_A \leq x_0 < x_1 < \dots < x_n \leq x_B = x_n + C_B \Delta x$$

where $C_A \in [0, 1]$ and $C_B \in [0, 1]$

- The grid points x_0 and x_n are not necessarily located on the boundaries x_A and x_B

Outflow: f_{n+p}

- f_{n+p} have to be defined, for $p = 1, \dots, 5$
- s^{th} order extrapolation procedure is used

$$f_{n+p} = f(u_{n+p}), \quad u_{n+p} = \sum_{j=1}^s u_{n-s+j} \prod_{\substack{l=1 \\ l \neq j}}^s \left(\frac{p+s-l}{j-l} \right)$$



M. GOLDBERG, *On a boundary extrapolation theorem by Kreiss*. 1977.

Outflow: f_{n+p}^x

- f_{n+p}^x have to be defined, for $p = 1, \dots, 4$
- Extension of the extrapolation procedure to the derivative

$$f_{n+p}^x = f'(u_{n+p}) \frac{\partial u}{\partial x} \Big|_{n+p},$$

$$\frac{\partial u}{\partial x} \Big|_{n+p} = \frac{1}{\Delta x} \sum_{j=1}^s u_{n-s+j} \prod_{\substack{l=1 \\ l \neq j}}^s \left(\frac{p+s-l}{j-l} \right) \sum_{\substack{q=1 \\ q \neq j}}^s \left(\frac{1}{p+s-q} \right)$$

Inflow: f_{-p}

- f_{-p} have to be defined, for $p = 1, \dots, 5$
- Inverse Lax-Wendroff (ILW) procedure is used
 - Taylor expansion at the boundary x_A

$$f_{-p} = f(u_{-p}), \quad u_{-p} = \sum_{k=0}^{s-1} \frac{(x_{-p} - x_A)^k}{k!} u^{*(k)},$$

where $u^{*(k)}$ are the $(s - k)^{\text{th}}$ order approximation of $\frac{\partial^k u}{\partial x^k} \Big|_{x_A}$

- Repetitive use of the PDE to convert spatial derivatives to time derivatives

$$u^{*(0)} = u(x_A, t) = g(t),$$

$$u^{*(1)} = \frac{\partial u}{\partial x} \Big|_{x_A} = -\frac{g'(t)}{f'(g(t))},$$

$$u^{*(2)} = \frac{\partial^2 u}{\partial x^2} \Big|_{x_A} = \frac{f'(g(t))g''(t) - 2f''(g(t))g'(t)^2}{f'(g(t))^3}.$$



S. TAN AND C.-W. SHU, *Inverse Lax-Wendroff procedure for numerical boundary conditions of conservation laws*. JCP, 2010.

Inflow: f_{-p}^x

- f_{-p}^x have to be defined, for $p = 1, \dots, 4$
- Extension of the ILW procedure to the derivative

$$f_{-p}^x = f'(u_{-p}) \frac{\partial u}{\partial x} \Big|_{-p},$$

$$\frac{\partial u}{\partial x} \Big|_{-p} = \sum_{k=0}^{s-2} \frac{(x_{-p} - x_A)^k}{k!} u^{*(k+1)}$$

where the $u^{*(k)}$ have already been computed in the evaluation of u_{-p}

Outcome

- Very heavy algebra for very high order of approximation, or for fully nonlinear systems of equations
- Simplified version of the ILW procedure with only to two leading terms



S. TAN, C. WANG, C.-W. SHU AND J. NING, *Efficient implementation of high order inverse Lax-Wendroff boundary treatment for conservation laws*. JCP, 2012.

Extension of the Simplified Inverse Lax-Wendroff (SILW)

- The first k_s moments are computed by the ILW procedure, and the following ones through the use of an extrapolation

$$u_{-p} = \sum_{k=0}^{k_s-1} \frac{(-p + C_A)^k}{k!} \Delta x^k u_{ILW}^{*(k)} + \sum_{k=k_s}^{s-1} \frac{(-p + C_A)^k}{k!} \Delta x^k u_{EXT}^{*(k)},$$

where the successive moments $u_{EXT}^{*(k)}$ write

$$u_{EXT}^{*(k)} = \sum_{j=1}^s \frac{u_{j-1}}{\Delta x^k} \prod_{\substack{l=1 \\ l \neq j}}^s \left(\frac{1 - C_A - l}{j - l} \right) \sum_{\substack{q_1=1 \\ q_1 \neq j}}^s \left(\frac{1}{1 - C_A - q_1} \right) \cdots \sum_{\substack{q_k=1 \\ q_k \neq j \\ q_k \neq q_1, \dots, q_{k-1}}}^s \left(\frac{1}{1 - C_A - q_k} \right)$$

- Same procedure on the derivative

$$\frac{\partial u}{\partial x} \Big|_{-p} = \sum_{k=0}^{k_s-2} \frac{(-p + C_A)^k}{k!} \Delta x^k u_{ILW}^{*(k+1)} + \sum_{k=k_s-1}^{s-2} \frac{(-p + C_A)^k}{k!} \Delta x^k u_{EXT}^{*(k+1)}$$

- 1 Introduction
- 2 Central Compact Schemes
- 3 Boundary conditions
- 4 G-K-S theory**
- 5 Eigenvalue spectrum
- 6 Conclusion

Theorem 1

G-K-S theory asserts that to show **stability** for the finite-domain problem, it is sufficient to show that **the inner scheme is Cauchy stable on $(-\infty, +\infty)$** , and that **each of the two quarter-plane problems is stable with the use of normal mode analysis**. Thus, the stability of the finite-domain problem is broken into the summation of three simpler problems

Theorem 2

For each quarter-plane problem that arise from Theorem 1, a **necessary and sufficient** condition for stability of the IBVP is that **no eigensolution exists**. This theorem is true for either the fully discrete case or the semidiscrete case.

References



B. GUSTAFSSON, H.-O. KREISS AND A. SUNDSTRÖM, *Stability theory of difference approximations for mixed initial boundary value problem. II*. Math. of Comp., 1972.



J.C. STRIKWERDA, *Initial boundary value problems for the method of lines*. JCP, 1980.

Quarter-plane problem

- We consider the following quarter-plane problem

$$\begin{cases} \frac{\partial u}{\partial t} + A \frac{\partial u}{\partial x} = 0, & x \geq 0, t \geq 0, \\ u(0, t) = g(t), & t \geq 0, \text{ if } \mathbf{A} > \mathbf{0}, \\ u(x, 0) = u_0(x), & x \geq 0, \\ \|u(\cdot, t)\| < \infty, \end{cases}$$

where $\|u(\cdot, t)\| = \int_0^\infty |u(x, t)|^2 dx$

- Uniform grid $0 \leq x_0 = C_0 \Delta x < x_1 < \dots$, $C_0 \in [0, 1]$
- The use of compact scheme yields the semidiscrete inner scheme

$$\mathcal{P} \frac{d u_j}{d t} = -\frac{A}{\Delta x} \mathcal{Q} u_j, \quad \text{for } j = r, r+1, \dots$$

where $\mathcal{P} = \sum_{i=-r_L}^{p_L} \alpha_i E^i$, $\mathcal{Q} = \sum_{i=-r_R}^{p_R} a_i E^i$, $E^i u_j = u_{j+i}$ and $r = \max(r_L, r_R)$

Quarter-plane problem

- Quarter-plane problem discretization

$$\left\{ \begin{array}{ll} \mathcal{P} \frac{d u_j}{d t} = -\frac{A}{\Delta x} Q u_j, & t \geq 0, \quad j = r, r+1, \dots \\ \mathcal{D}_j \frac{d u_j}{d t} = -\frac{A}{\Delta x} B_j u_j + \tilde{g}_j(t), & t \geq 0, \quad j = 0, 1, \dots, r-1 \\ u_j(0) = u_0(x_j), & j = 0, 1, \dots \\ \sum_{j=0}^{\infty} |u_j(t)|^2 \Delta x < \infty, & t \geq 0 \end{array} \right.$$

Definition

An eigensolution is the nontrivial function $v(x, s) = e^{st}\phi(x)$, which satisfies

- $s \Delta x \mathcal{P} v_j + A Q v_j = 0, \quad j = r, r+1, \dots$
- $Re(s) \geq 0$
- For $Re(s) > 0$, $v(x, s)$ is bounded as $x \rightarrow \infty$
- For $Re(s) = 0$, $v(x, s) = \lim_{\varepsilon \rightarrow 0^+} v(x, s + \varepsilon)$, where $v(x, s + \varepsilon)$ satisfies a) and c) with respect with $s + \varepsilon$
- $s \Delta x \mathcal{D}_j v_j + A B_j v_j = \tilde{g}_j(t), \quad j = 0, 1, \dots, r-1$

Example: CCS-T6

- Inner scheme

$$-\frac{u_{j-2}^x}{12} + u_j^x - \frac{u_{j+2}^x}{12} = \frac{16}{9} \frac{u_{j+1} - u_{j-1}}{2\Delta x} - \frac{17}{18} \frac{u_{j+2} - u_{j-2}}{4\Delta x}$$

- u_{-p} and u_{-p}^x , for $p = 1, 2$, are evaluated by extrapolation in the outflow case, and ILW or SILW in the inflow case

Normal mode analysis: $u_j(t) = e^{st} \phi_j$ where $\phi_j = C K^j$

- Characteristic equation, with $\tilde{s} = s \frac{\Delta x}{|A|}$

$$\tilde{s} \left(K^2 - \frac{1}{12} (K^4 + 1) \right) + \operatorname{sgn}(A) \left(\frac{16}{18} (K^3 - K) - \frac{17}{72} (K^4 - 1) \right) = 0$$

- Only two roots of the resolvent equation yield $|K| \leq 1$
- Thus, the general solution has the form

$$\phi_j = C_1 K_1^j + C_2 K_2^j,$$

where K_1, K_2 the two roots with $|K| < 1$ and C_1, C_2 two constants

Boundary conditions

- Substituting the general solution into the two boundary conditions for $j = 0$ and $j = 1$ yield a 2×2 system of equations
- For example, in the outflow case ($A = -1$) with extrapolation boundary

$$\tilde{s}(72\phi_0 - 6\phi_2) + \frac{1647}{10}\phi_0 - 363\phi_1 + 358\phi_2 - 234\phi_3 + \frac{177}{2}\phi_4 - \frac{71}{5}\phi_5 = 0$$

$$\tilde{s}(72\phi_1 - 6\phi_3) - \frac{71}{5}\phi_0 + \frac{159}{2}\phi_1 - 150\phi_2 + 74\phi_3 - 21\phi_4 + \frac{33}{10}\phi_5 = 0$$

- This system has only a trivial solution unless its determinant is null

Outcome

- The **extrapolation outflow** boundary condition maintain the stability for any CCS and any value of C_0 (no eigensolution)
- The **ILW inflow** boundary condition maintain the stability for any CCS and any value of C_0 (no eigensolution)
- The stability of the CCS with the **SILW inflow** boundary condition **depends on** the value of C_0 and on the **number of leading terms** k_S

CCS-T6 provided with SILW inflow boundary

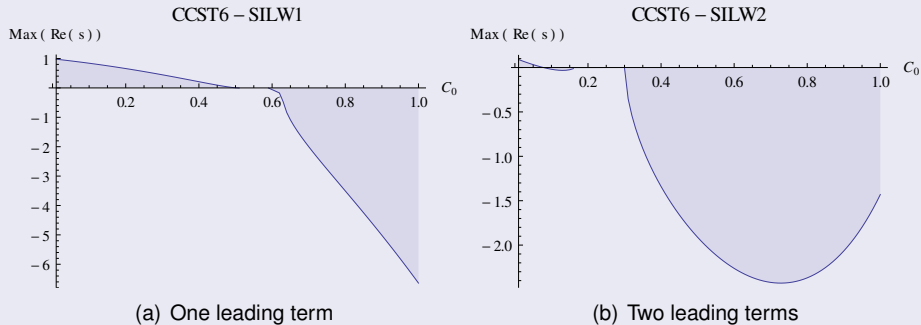


Figure : Maximum of the real part of the eigenvalues as function of C_0 for the CCS-T6 scheme with the SILW boundary condition with one and two leading terms.

CCS-T6 provided with SILW inflow boundary

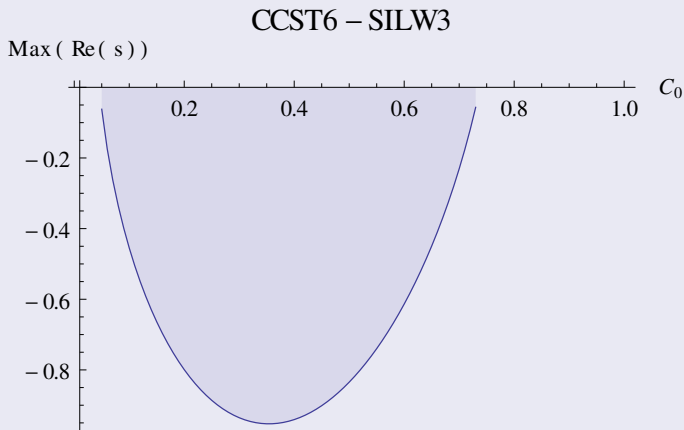


Figure : Maximum of the real part of the eigenvalues as function of C_0 for the CCS-T6 scheme with the SILW boundary condition with three leading terms.

Time discretization

- We use the third-order TVD Runge-Kutta method
- Let us consider the general system

$$\frac{d u}{d t} = F(t, u)$$

- We derive the eigenvalue problem setting $F(t, u) = s u$

$$u^{n+1} = \left(1 + \mu + \frac{\mu^2}{2} + \frac{\mu^3}{6}\right) u^n,$$

where $u^n = u(x, t^n)$ and $\mu = s \Delta t = \tilde{s} \frac{|A| \Delta t}{\Delta x}$

- This is nothing but a Taylor expansion of the exponential e^μ
- Assuming a solution of the form $u^n = z^n u^0$, where z is a complex number, the stability domain of the considered time discretization writes

$$|z(\mu)| \leq 1, \quad \text{where} \quad z(\mu) = 1 + \mu + \frac{\mu^2}{2} + \frac{\mu^3}{6}$$

Normal mode analysis

- Semidiscrete case: $u_j(t^{n+1}) = e^{s \Delta t} u_j(t^n) = e^{\tilde{s} \frac{|A| \Delta t}{\Delta x}} u_j(t^n)$
 $Re(s) \leq 0$ and s is not a generalized eigenvalue \implies Stability
- Fully discrete case: $u_j^{n+1} = z(s \Delta t) u_j^n = z(\tilde{s} \frac{|A| \Delta t}{\Delta x}) u_j^n$
 $|z| \leq 1$ and z is not a generalized eigenvalue \implies Stability
- We introduce the CFL condition: $CFL = \frac{|A| \Delta t}{\Delta x}$
- We substitute in the time discretization resolvent equation the eigenvalues \tilde{s} we have found in the semidiscrete G-K-S analysis

Procedure

- We start the stability analysis with the same CFL condition than for the periodic boundary case
- If the fully discrete scheme is not stable under this CFL ($\exists z, |z| \geq 1$), we use a decreasing sequence of CFL condition, re-performing at each step to stability analysis

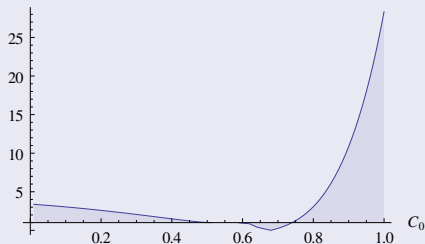
Outcome

- The **extrapolation outflow** boundary condition maintain the stability for any RK3-CCS and any value of C_0 (no eigensolution), **under the same CFL** than for the periodic boundary case
- The **ILW inflow** boundary condition maintain the stability for any RK3-CCS and any value of C_0 (no eigensolution), **under the same CFL** than for the periodic boundary case
- The stability of the CCS with the **SILW inflow** boundary condition **depends on** the value of C_0 and of the **number of leading terms** k_s . The fully discrete scheme would be **stable under the same CFL** than for the periodic boundary case **or not stable for any CFL**, depending on the number of leading terms

RK3-CCST6 provided with SILW inflow boundary

CCST6 – SILW1

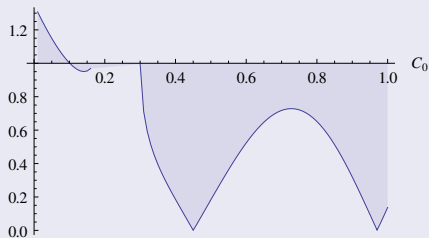
$\max(\text{Abs}(z))$



(a) One leading term

CCST6 – SILW2

$\max(\text{Abs}(z))$



(b) Two leading terms

Figure : Maximum of the absolute value of the eigenvalues as function of C_0 for the RK3-CCST6 scheme with the SILW boundary condition with one and two leading terms.

RK3-CCST6 provided with SILW inflow boundary

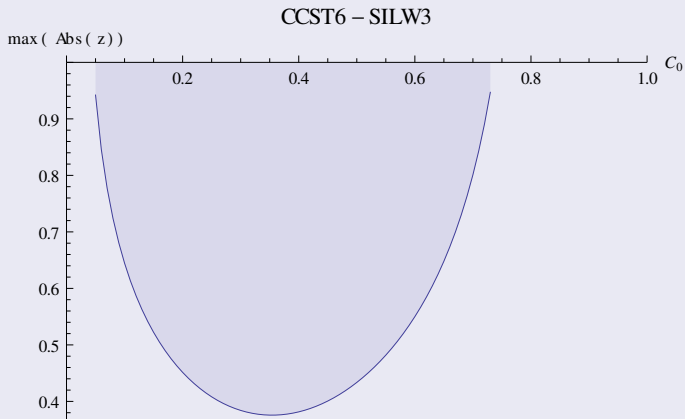


Figure : Maximum of the absolute value of the eigenvalues as function of C_0 for the RK3-CCST6 scheme with the SILW boundary condition with three leading terms.

G-K-S theory advantages

- Analytical analysis of the stability
- The stability of the finite-domain problem is broken into the summation of three simpler problems
- Analysis independent of the mesh resolution

G-K-S theory disadvantages

- Complex theory
- **Very heavy algebra** (not practical for very high-order of accuracy)

- 1 Introduction
- 2 Central Compact Schemes
- 3 Boundary conditions
- 4 G-K-S theory
- 5 Eigenvalue spectrum**
- 6 Conclusion

Initial Boundary Value Problem

- We consider the following initial boundary value problem

$$\begin{cases} \frac{\partial u}{\partial t} + A \frac{\partial u}{\partial x} = 0, & x \in [x_A, x_B], t \geq 0, \\ u(x_A, t) = g(t), & t \geq 0, \\ u(x, 0) = u_0(x), & x \in [x_A, x_B], \end{cases}$$

- We assume $A > 0$

Cartesian grid

- Uniform mesh $\{x_j\}_{j=0, \dots, n}$ such as

$$x_0 - C_A \Delta x = x_A \leq x_0 < x_1 < \dots < x_n \leq x_B = x_n + C_B \Delta x$$

where $C_A \in [0, 1]$ and $C_B \in [0, 1]$

- The grid points x_0 and x_n are not necessarily located on the boundaries x_A and x_B

Discretization

- Central compact scheme is used at the inner points
- The ghost points located at the outflow boundary condition are evaluated by an extrapolation procedure
- The ghost points located at the inflow boundary condition are evaluated either by the ILW procedure or its simplified version SILW
- Finally, the semidiscrete scheme yields a linear system of equations expressed in a matrix-vector form as

$$P \frac{d\mathbf{U}}{dt} = -\frac{A}{\Delta x} Q \mathbf{U},$$

where P is invertible and $\mathbf{U} = (u_0, u_1, \dots, u_n)^t$

Normal mode analysis

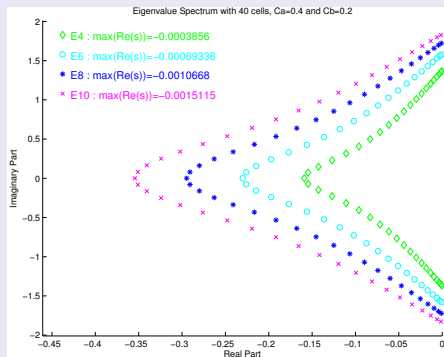
- Assuming a solution of the form $u(x, t) = e^{st} u^0(x)$, the semidiscrete scheme yields

$$\tilde{s} P \mathbf{U} = -\text{sgn}(A) Q \mathbf{U},$$

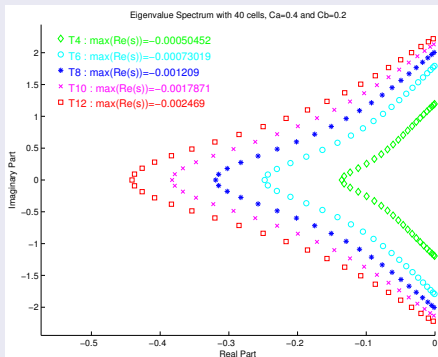
where $\tilde{s} = s \frac{\Delta x}{|A|}$ being the considered eigenvalue

- Thus, we compute the eigenvalues of matrix $-\text{sgn}(A) P^{-1} Q$
- As previously, the semidiscrete scheme provided with the considered boundary conditions, on the studied mesh, is stable if the whole eigenvalue spectrum lies in the left-hand plane ($\text{Re}(\tilde{s}) \leq 0$)

CCS provided with extrapolation-ILW boundary conditions



(a) CCS-E



(b) CCS-T

Figure : The eigenvalue spectrum of the semi-discrete central compact schemes, closed with an Inverse Lax-Wendroff procedure for the inflow boundary, and extrapolation for the outflow boundary, with 40 cells and $C_A = 0.4$ and $C_B = 0.2$.

CCS-P provided with extrapolation-ILW boundary conditions

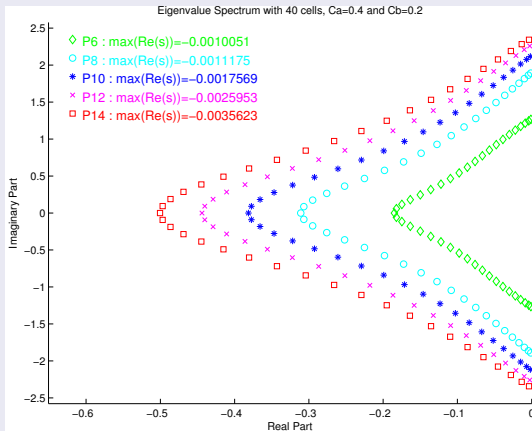


Figure : The eigenvalue spectrum of the semi-discrete CCS-P schemes, closed with an Inverse Lax-Wendroff procedure for the inflow boundary, and extrapolation for the outflow boundary, with 40 cells and $C_A = 0.4$ and $C_B = 0.2$.

CCS-T6 provided with extrapolation-SILW1 boundary conditions

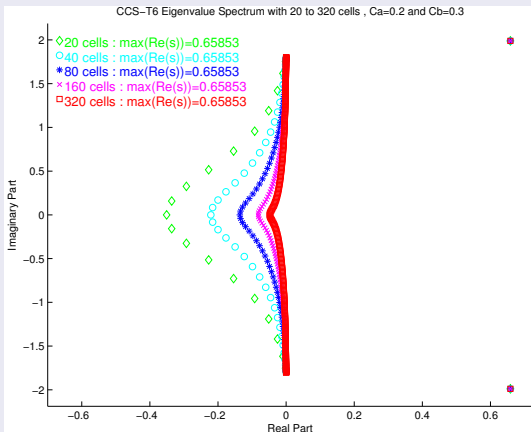


Figure : The eigenvalue spectrum of the CCS-T6, provided with SILW procedure with one term for the inflow boundary, and extrapolation for the outflow boundary, with $C_A = 0.2$.

CCS-T6 provided with extrapolation-SILW1 boundary conditions

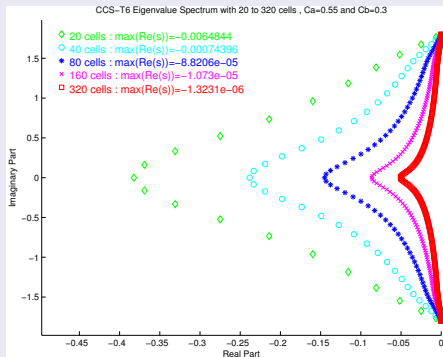
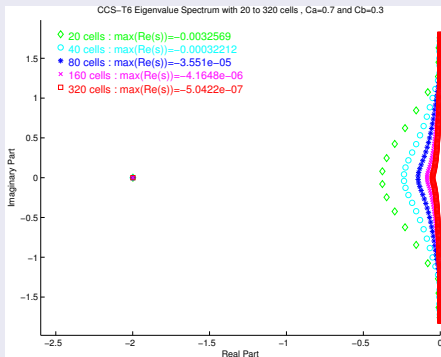
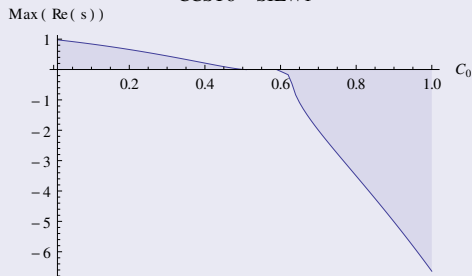
(a) $C_A = 0.55$ (b) $C_A = 0.7$

Figure : The eigenvalue spectrum of the CCS-T6, provided with SILW procedure with one term for the inflow boundary, and extrapolation for the outflow boundary.

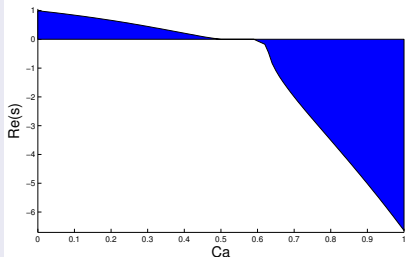
CCS-T6 provided with extrapolation-SILW1 boundary conditions

CCST6 – SILW1



(a) G-K-S analysis

Particular eigenvalue real part of CCST6–SILW1



(b) Eigenspectrum analysis

Figure : Real part of the eigenvalues responsible of instability of the CCS-T6 scheme provided with extrapolation and SILW1 boundary conditions.

CCS-T6 provided with extrapolation-SILW2 boundary conditions

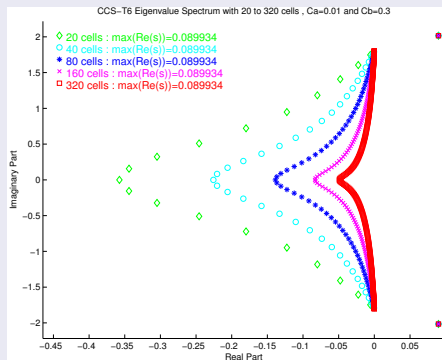
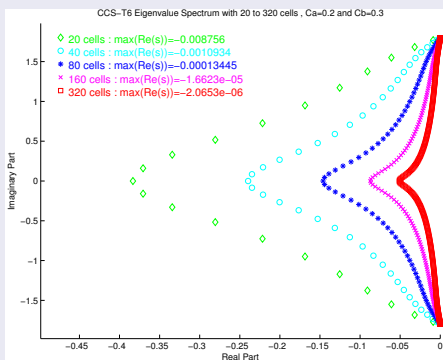
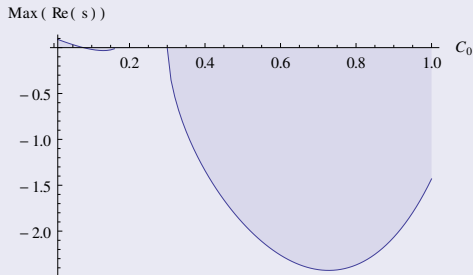
(a) $C_A = 0.01$ (b) $C_A = 0.2$

Figure : The eigenvalue spectrum of the CCS-T6, provided with SILW procedure with two terms for the inflow boundary, and extrapolation for the outflow boundary.

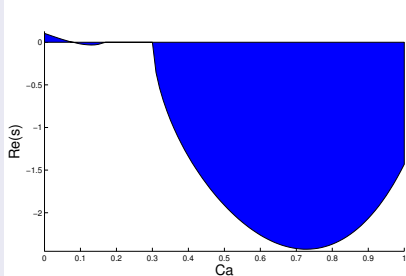
CCS-T6 provided with extrapolation-SILW2 boundary conditions

CCST6 – SILW2



(a) G-K-S analysis

Particular eigenvalue real part of CCST6–SILW2



(b) Eigenspectrum analysis

Figure : Real part of the eigenvalues responsible of instability of the CCS-T6 scheme provided with extrapolation and SILW2 boundary conditions.

CCS-T6 provided with extrapolation-SILW3 boundary conditions

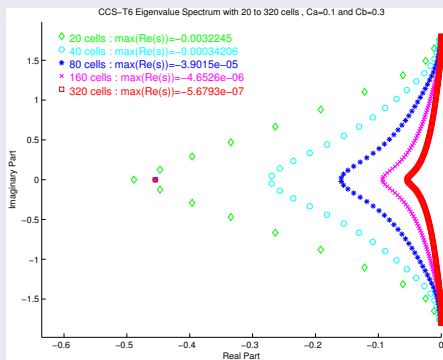
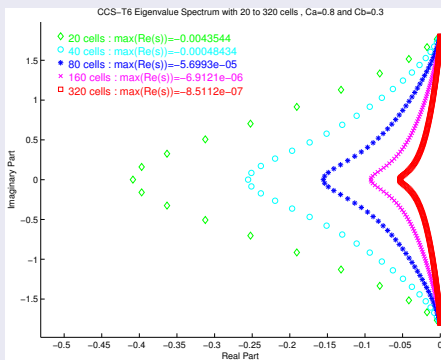
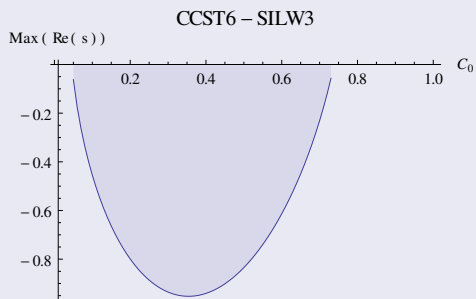
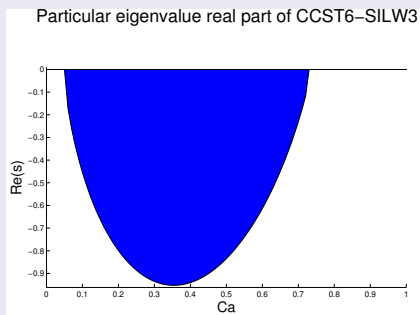
(a) $C_A = 0.1$ (b) $C_A = 0.8$

Figure : The eigenvalue spectrum of the CCS-T6, provided with SILW procedure with three terms for the inflow boundary, and extrapolation for the outflow boundary.

CCS-T6 provided with extrapolation-SILW3 boundary conditions



(a) G-K-S analysis



(b) Eigenspectrum analysis

Figure : Real part of the eigenvalues responsible of instability of the CCS-T6 scheme provided with extrapolation and SILW3 boundary conditions.

Outcome

- The CCS semidiscrete schemes provided with **extrapolation outflow** boundary condition and **ILW inflow** boundary condition are stable for any CCS and values of C_A and C_B
- The stability of the CCS provided with **extrapolation outflow** boundary condition and **SILW inflow** boundary condition **depends on** the values of C_A and C_B and on the **number of leading terms** k_s
- For some specific value of C_A , the eigenvalue spectrum of CCS provided with extrapolation and simplified inverse Lax-Wendroff boundaries may present some particular eigenvalues independent of the resolution
- These particular eigenvalues correspond to the solution of the eigenvalue problem solved in the G-K-S stability analysis
- Since the extrapolation boundary brings no instability, the two different approaches lead to the same results

Discretization

- We recall the semidiscrete system obtained previously

$$P \frac{d\mathbf{U}}{dt} = -\frac{A}{\Delta x} Q \mathbf{U}$$

- We apply to this ODE the third-order TVD Runge-Kutta method
- Doing so, the fully discretize problem can be written as

$$\mathbf{U}^{n+1} = G \mathbf{U}^n,$$

where \mathbf{U}^n and \mathbf{U}^{n+1} are the solution vectors at time t^n and t^{n+1}

- The operator G writes

$$G = I_d - \operatorname{sgn}(A) \frac{|A| \Delta t}{\Delta x} P^{-1} Q + \left(\frac{|A| \Delta t}{\Delta x} \right)^2 (P^{-1} Q)^2 - \operatorname{sgn}(A) \left(\frac{|A| \Delta t}{\Delta x} \right)^3 (P^{-1} Q)^3,$$

where I_d is the identity matrix

Normal mode analysis

- Assuming a solution of form $u^n = z^n u^0$, the eigenvalue problem writes

$$z \mathbf{U}^n = \mathbf{G} \left(\frac{|A| \Delta t}{\Delta x} \right) \mathbf{U}^n$$

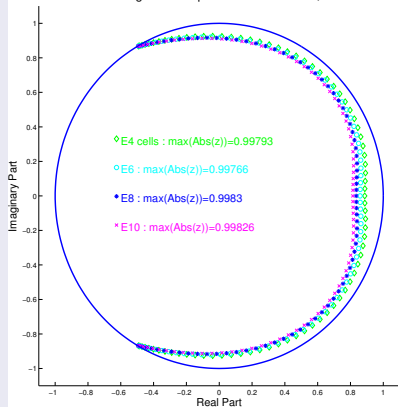
- We set the condition $CFL = \frac{|A| \Delta t}{\Delta x}$
- We compute the eigenvalues of matrix $\mathbf{G}(CFL)$
- The fully discrete scheme provided with the considered boundary conditions, on the studied mesh, is stable if the whole eigenvalue spectrum lies in the unit circle

Procedure

- We start the stability analysis with the same CFL condition than for the periodic boundary case
- If the fully discrete scheme is not stable under this CFL ($\exists z, |z| \geq 1$), we use a decreasing sequence of CFL condition, re-computing at each step the eigenvalues

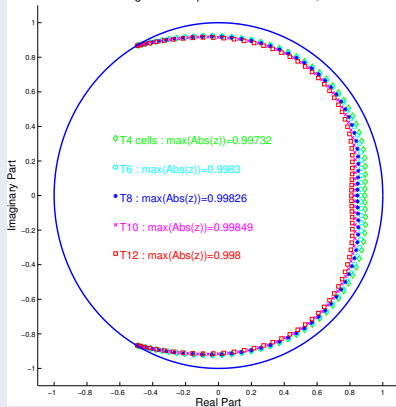
RK3-CCS provided with extrapolation-ILW boundary conditions

RK3-CCSE Discrete Eigenvalue Spectrum with 80 cells, $C_a=0.3$ and $C_b=0.3$



(a) CCS-E

RK3-CCST Discrete Eigenvalue Spectrum with 80 cells, $C_a=0.3$ and $C_b=0.3$



(b) CCS-T

Figure : The eigenvalue spectrum of the RK3-CCS, closed with an Inverse Lax-Wendroff procedure for the inflow boundary, and extrapolation for the outflow boundary, with 40 cells and $C_A = 0.3$ and $C_B = 0.3$.

RK3-CCSP provided with extrapolation-ILW boundary conditions

RK3-CCSP Discrete Eigenvalue Spectrum with 80 cells , $C_A=0.3$ and $C_B=0.3$

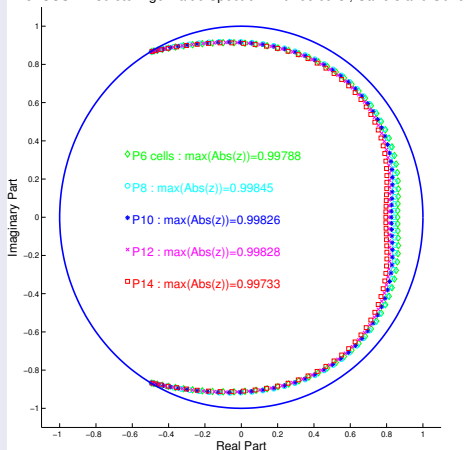


Figure : The eigenvalue spectrum of the RK3-CCSP, closed with an Inverse Lax-Wendroff procedure for the inflow boundary, and extrapolation for the outflow boundary, with 40 cells and $C_A = 0.3$ and $C_B = 0.3$.

RK3-CCST6 with extrapolation-SILW1 boundary conditions

RK3-CCST6 Discrete Eigenvalue Spectrum with 40 to 320 cells, $C_a=0.2$ and $C_b=0.3$

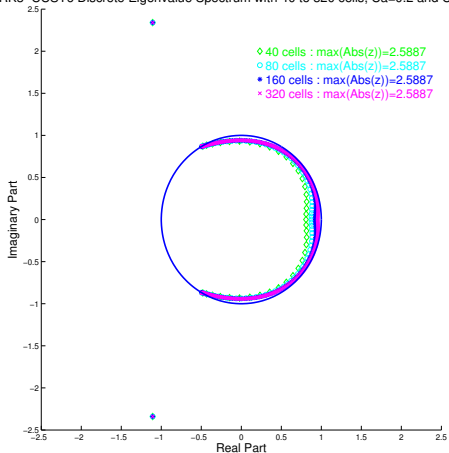
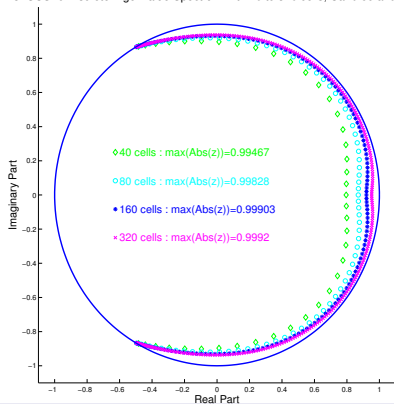


Figure : The eigenvalue spectrum of the RK3-CCST6, provided with SILW procedure with one term for the inflow boundary, and extrapolation for the outflow boundary, with $C_A = 0.2$.

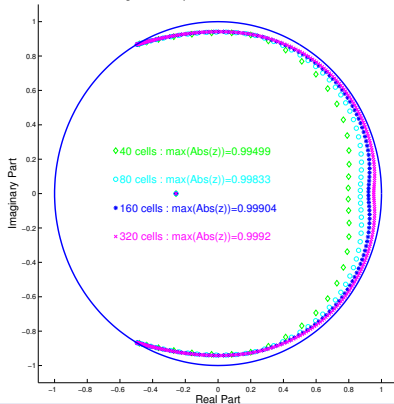
RK3-CCST6 with extrapolation-SILW1 boundary conditions

RK3-CCST6 Discrete Eigenvalue Spectrum with 40 to 320 cells, $Ca=0.55$ and $Cb=0.3$



(a) $C_A = 0.55$

RK3-CCST6 Discrete Eigenvalue Spectrum with 40 to 320 cells, $Ca=0.7$ and $Cb=0.3$



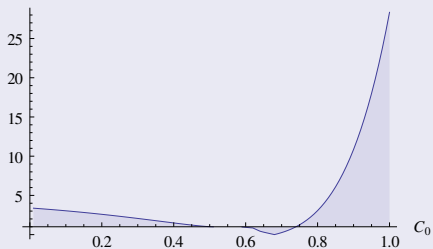
(b) $C_A = 0.7$

Figure : The eigenvalue spectrum of the RK3-CCST6, provided with SILW procedure with one term for the inflow boundary, and extrapolation for the outflow boundary.

RK3-CCST6 with extrapolation-SILW1 boundary conditions

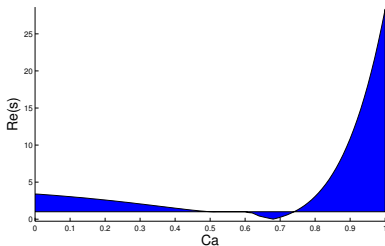
CCST6 – SILW1

$\max(\text{Abs}(z))$



(a) G-K-S analysis

Particular eigenvalue absolute value of CCST6–SILW1

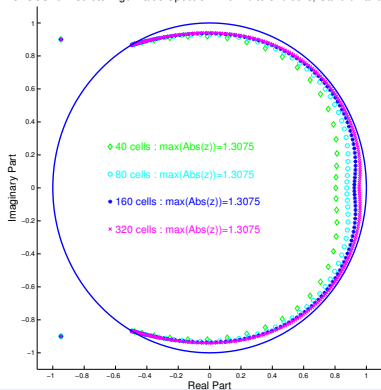


(b) Eigenspectrum analysis

Figure : Real part of the eigenvalues responsible of instability of the RK3-CCST6 scheme provided with extrapolation and SILW1 boundary conditions.

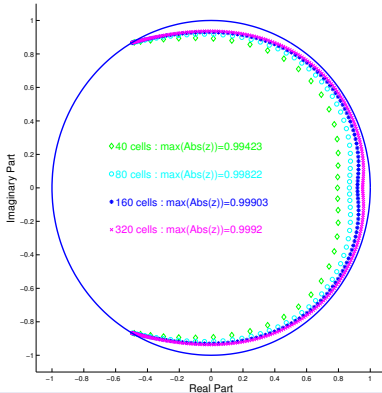
RK3-CCST6 with extrapolation-SILW2 boundary conditions

RK3-CCST6 Discrete Eigenvalue Spectrum with 40 to 320 cells, $C_A=0.01$ and $C_b=0.3$



(a) $C_A = 0.01$

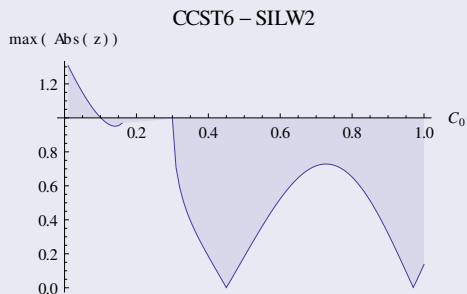
RK3-CCST6 Discrete Eigenvalue Spectrum with 40 to 320 cells, $C_A=0.2$ and $C_b=0.3$



(b) $C_A = 0.2$

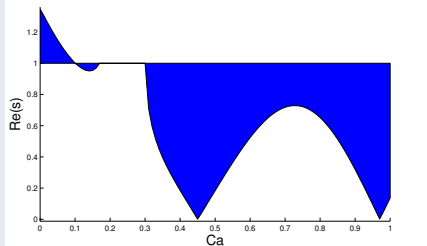
Figure : The eigenvalue spectrum of the RK3-CCST6, provided with SILW procedure with two terms for the inflow boundary, and extrapolation for the outflow boundary.

RK3-CCST6 with extrapolation-SILW2 boundary conditions



(a) G-K-S analysis

Particular eigenvalue absolute value of CCST6–SILW2

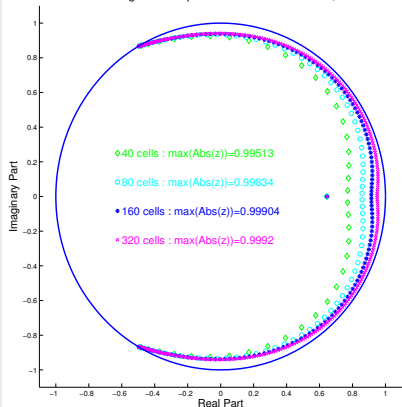


(b) Eigenspectrum analysis

Figure : Real part of the eigenvalues responsible of instability of the RK3-CCST6 scheme provided with extrapolation and SILW2 boundary conditions.

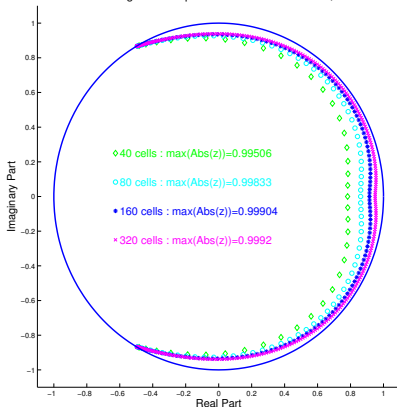
RK3-CCST6 with extrapolation-SILW3 boundary conditions

RK3-CCST6 Discrete Eigenvalue Spectrum with 40 to 320 cells, $Ca=0.1$ and $Cb=0.3$



(a) $C_A = 0.1$

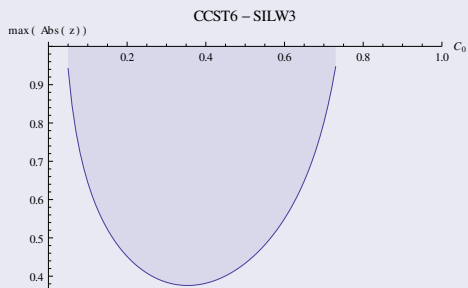
RK3-CCST6 Discrete Eigenvalue Spectrum with 40 to 320 cells, $Ca=0.8$ and $Cb=0.3$



(b) $C_A = 0.8$

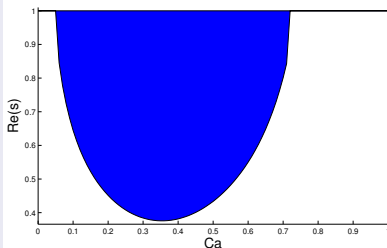
Figure : The eigenvalue spectrum of the RK3-CCST6, provided with SILW procedure with three terms for the inflow boundary, and extrapolation for the outflow boundary.

RK3-CCST6 with extrapolation-SILW3 boundary conditions



(a) G-K-S analysis

Particular eigenvalue absolute value of CCST6–SILW3



(b) Eigenspectrum analysis

Figure : Real part of the eigenvalues responsible of instability of the RK3-CCST6 scheme provided with extrapolation and SILW3 boundary conditions.

Outcome

- The RK3-CCS schemes provided with **extrapolation outflow** boundary condition and **ILW inflow** boundary condition are stable for any CCS and values of C_A and C_B
- The stability of the RK3-CCS schemes provided with **extrapolation outflow** boundary condition and **SILW inflow** boundary condition **depends on** the values of C_A and C_B and on the **number of leading terms** k_S
- For some specific value of C_A , the eigenvalue spectrum of RK3-CCS provided with extrapolation and simplified inverse Lax-Wendroff boundaries may present some particular eigenvalues independent of the resolution
- These particular eigenvalues correspond to the solution of the eigenvalue problem solved in the G-K-S stability analysis
- Since the extrapolation boundary brings no oscillations, the two different approaches lead to the same results

Number of terms required in the SILW procedure

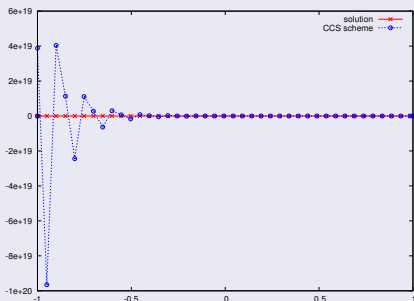
Scheme	Leading terms
CCS-E4	3
CCS-E6	4
CCS-E8	5
CCS-E10	5

Scheme	Leading terms
CCS-T4	3
CCS-T6	3
CCS-T8	5
CCS-T10	8
CCS-T12	9

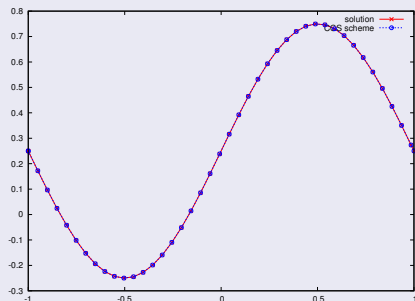
Scheme	Leading terms
CCS-P6	4
CCS-P8	5
CCS-P10	7
CCS-P12	9
CCS-P14	9

Table : Minimum numbers of leading terms required by the different RK3-CCS schemes to remain stable under the same CFL than for periodic boundary conditions.

Linear advection case with $C_A = 0.001$ and $C_B = 0.3$



(a) Two leading terms, $t = 10$



(b) Three leading terms, $t = 10000$

Figure : Numerical results obtained with RK3-CCST6 scheme provided with extrapolation and SILW boundaries in the linear advection case ($A = 1$) on $x \in [-1, 1]$, with the initial and boundary condition $u_0(x) = 0.25 + 0.5 \sin(\pi x)$ and $u(-1, t) = 0.25 - 0.5 \sin(\pi(1 + t))$, with 40 cells and $CFL = 0.96$.

- 1 Introduction
- 2 Central Compact Schemes
- 3 Boundary conditions
- 4 G-K-S theory
- 5 Eigenvalue spectrum
- 6 Conclusion**

Conclusions

- Both G-K-S and eigenspectrum stability analysis have been done, and gave **perfectly consistent results**
- CCS have been proved to remain stable under the same CFL than the periodic boundaries case and for any boundary position, provided with
 - outflow extrapolation boundary
 - inflow inverse Lax-Wendroff boundary
- The number of leading terms required by the SILW procedure for the central compact scheme to remain stable has been determined

Perspectives

- Design an energy stability
- Adapt CCS and ILW to the SBP-SAT operators
- Apply the studied schemes and boundaries to more practical applications (Euler, Navier-Stokes, . . .)



M.H. CARPENTER, D. GOTTLIEB AND S. ABARBANEL, *Time-stable conditions for finite-difference schemes solving hyperbolic systems: methodology and application to high-order compact schemes*. JCP, 1994.